1st Croatian Conference on Earthquake Engineering
1CroCEE
22-24 March 2021 Zagreb, Croatia

DOI: https://doi.org/10.5592/CO/1CroCEE.2021.190

Review of cyclic soil behavior and input parameters for seismic site response analyses and liquefaction

Mladen Vucetic

Professor Emeritus and Reserch Professor, Civil and Environmental Eng. Department, University of California, Los Angeles - UCLA, USA, *vucetic@g.ucla.edu*

Abstract

During earthquakes soil deposits are exposed to all kinds of seismic waves and are consequently subjected to three-directional cyclic loading and straining. In the geotechnical earthquake engineering practice, however, the analyses of such complex response of the deposits to seismic forces, the site response analyses, are typically reduced to the analyses of the effects of the vertically propagating plane shear waves through horizontally layered deposits. The popular geotechnical laboratory tests for simulation of such behavior are cyclic simple shear, cyclic triaxial, cyclic torsional and resonant column tests that all cyclically shear the soil specimen in just one direction, typically in series of cycles with constant amplitude of shear stress, τ_c, or shear strain, γ_c. The paper presents several fundamental aspects of the cyclic soil behavior obtained relatively recently in the cyclic simple shear tests, indicating that the basic research of cyclic and dynamic soil properties is still going on. The parameters and curves derived from cyclic simple shear tests that are used in popular computer models for site response analyses that are treated in this paper include: maximum shear modulus, G_{max}, cyclic secant shear modulus, Gs, equivalent viscous damping ratio, λ, curve of the reduction of the first cycle G_s with γ_c, second cycle λ versus γ_c curve, pore water pressure change with the number of cycles N in saturated soils, change of Gs with N, and the cyclic threshold shear strains for pore water pressure change, γ_{tp}, and cyclic degradation, γ_{td}.

Key words: soil, earthquakes, cyclic loading, shear modulus, damping, strain rate, frequency, threshold strain, cyclic degradation, cyclic pore water pressure, simple shear testing

1 Input parameters for seismic site response analyses

The response of civil engineering structures to seismic shaking depends on the complex 3-dimensional cyclic stress-strain properties and behavior of soils in subsurface layers due to 3-directonal loading. In practice, however, it is typical to consider just vertical propagation of plane shear waves through horizontally layered soil deposit such hat the soil's stress-strain conditions are those of pure shear stresses, τ, and associated shear strains, γ, applied cyclically in just one direction on top of the existing vertical and horizontal effective stresses σ_{vc}' and σ_{hc}'. Under such conditions the stress-strain behavior is described by cyclic loops that can be obtained from one-directional cyclic loading tests, such as cyclic simple shear, cyclic triaxial, cyclic torsional and resonant column. In these tests soil is typically subjected to series of cycles with constant amplitude of shear stress, τ_c, or shear strain, γ_c. The test that most directly simulates the cyclic pure shear stress conditions is the cyclic simple shear test [1]. In this paper the results obtained relatively recently in the cyclic simple shear devices in the soil dynamics laboratory at the University of California, Los Angeles, are presented and discussed. One of the testing devices used is presented in Figure 1.

The seismic site response analyses are performed with various computer models, such as SHAKE [4], DESRA-2 [5] and its modifications [6, 7], and DEEPSOIL [30]. In these computer codes, the soil material input parameters for each layer include the parameers and curves listed in the Abstract and treated below, so the knowledge gained from the test results presented is of practical significance because it can be employed to improve the performance of these codes.

The idealized 1st and a quarter cycles loop is presnted in Figure 2. In Figure 3 are presented the second cycle loop and the two loops from a single test, the loop in the first cycle and cycle N. The parameters and curves describing the cyclic behavior presented by these loops are the variation of the 1st cycle loops with amplitude, γ_c, typically presented by the curves G_s-logγ_c, G_s/G_{max}-logγ_c, and λ-logγ_c. Furthermore, the change of soil stiffness under the cyclic strain-controlled shearing with constant γ_c in each cycle N can be described with the stiffness index, δ_N, that measures the relative change of G_S in cycle N, G_{SN}, with respect to the initial modulus G_{S1} in the first cycle N=1: $\delta_N = G_{SN}/G_{S1} = \tau_{cN}/\tau_{c1}$.

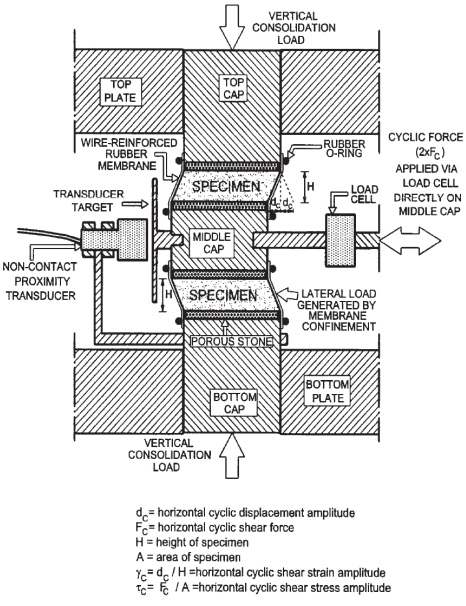

Figure 1. Setup of specimens in the UCLA dual-specimen DSS device (DSDSS device) for small-strain testing [2, 3]

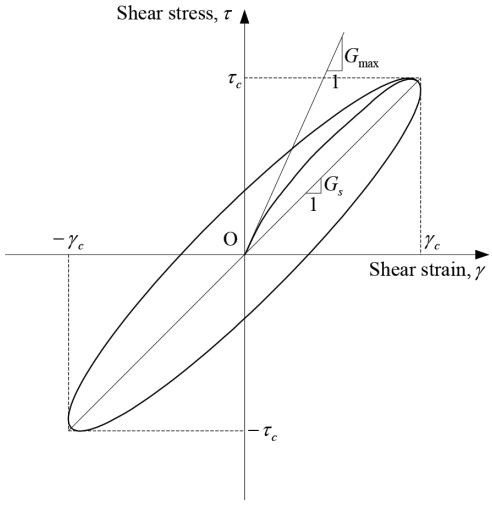

Figure 2. Idealized fully closed initial cyclic stress-strain loop (first 1.25 cycles) with definition of Gs and G_{max}

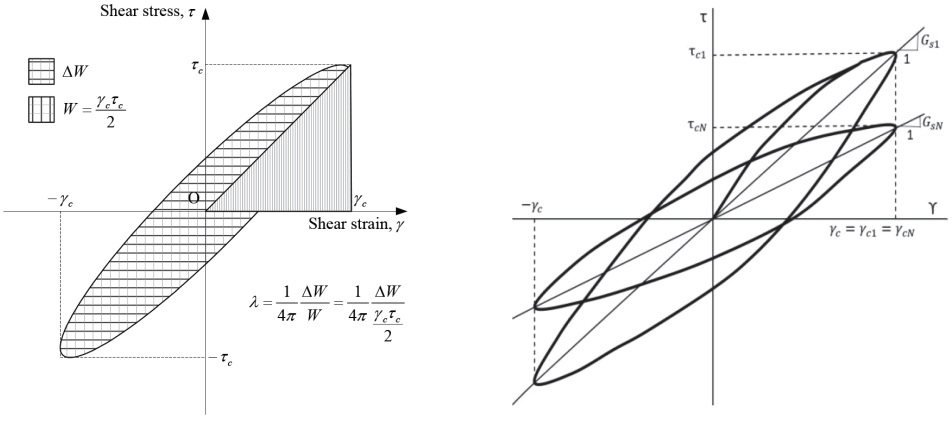

Figure 3. Definition of the equivalent viscous damping ratio, λ and sketch of the idealized cyclic strain-controlled behavior in the first cycle, N=1, and a subsequent cycle N

2 Effects of the rate of shear straining and frequency on GS, GS/G_{max}-log γ_c curve, λ, and λ-log γ_c curve

The parameters G_s and λ and the G_s-logγ_c, G_s/G_{max}-logγ_c, and λ-logγ_c curves are affected by many factors. One of them is the rate of shear straining $\dot{\gamma} = d\gamma/dt$. The effects of $\dot{\gamma}$ encompass those of the frequency of cyclic loading, *f*, level of the average strain rate in a single unifiorm cycle, $\dot{\gamma}=4\gamma_c/T=4f\gamma_c$, where T is the cycle period, and the variation of the rate in a single cycle. How at a given γ_c the slope of the cyclic loop G_s changes with $\dot{\gamma}$ is sketched in Figure 4. At a given γ_c, modulus G_s increases approximately linearly with the logarithm of average $\dot{\gamma}$ and associated *f*. This increase can be quantified with the strain-rate shear modulus factor $N_{\dot{\gamma}\text{-}G}$ [8] which describes the relative increase of $(G_s)_{low f}$ due to the tenfold increases of $\dot{\gamma}$. Figure 5 provides the rate-of-straining effect on G_s obtained for many different soils. Two trends can be observed: (1) for any level of γ_c factor $N_{\dot{\gamma}\text{-}G}$ increases consistently with PI, and (2) the rate-of-straining effect increases as γ_c gets smaller.

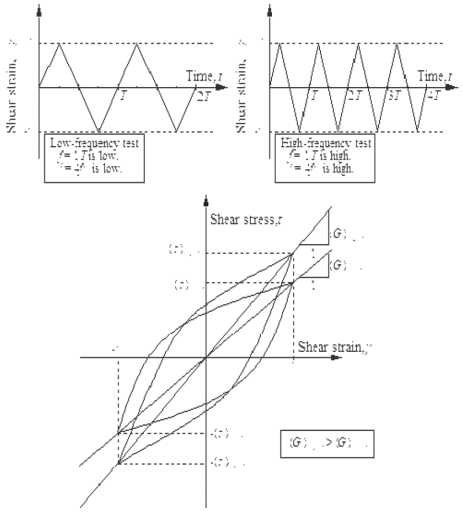

Figure 4. Effect of the frequency and associated average strain rate on cyclic loading behavior

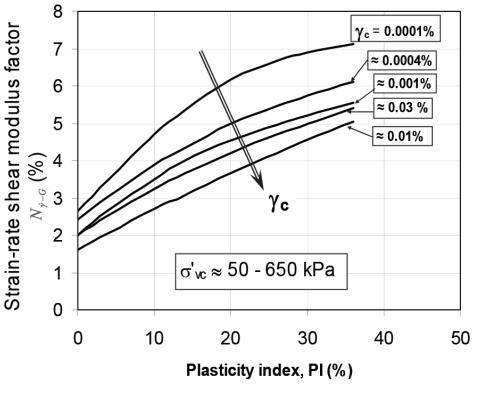

Figure 5. General trends of the strain-rate shear modulus factor with PI and γ_c (from [9, 10, 11, 12])

From Figure . 5 it is also evident that the shapes of the G_s/G_{max}-logγ_c curves must depend on the frequency, *f*, and associated average strain rate, $\dot{\gamma}$. In this context two types of G_s/G_{max}-logγ_c curves can be constructed: curves obtained from tests with the same *f* at all γ_c levels, and curves from tests with constant $\dot{\gamma}$ at all γ_c levels. Depending on whether $\dot{\gamma}$ or *f* is constant, different curvatures of modulus reduction curves are obtained. If $\dot{\gamma}$ is constant, G_s consistently decreases with γ_c. If *f* is constant, G_s decreases with γ at higher γ_c, but at low γ_c it may for clays increase and then decrease, which means that at

low γ_c the G_s/G_{max}-logγ_c curve for clay may run above G_s/G_{max}=1.0 line. These trends are reported in [8, 9, 13]. How constant *f* and $\dot{\gamma}$ curves compare for different soils is indicated in Figure . 6. The G_s/G_{max}-logγ_c curves derived from the results of DSDSS tests (Figure . 1) on a natural sandy soil (labeled Arlita-1) and a natural clay having PI=26 (labeled ESC-1) are compared. For sandy soil, the curves for two constant frequencies, *f* =0.3 Hz and 3 Hz, and the curves for constant values of $\dot{\gamma}$ ranging between 0.0001 %/sec and 0.003 %/sec, plot practically on top of each other. This is because sandy soils do not exhibit noticeable effects of the rate of straining. In the case of clay, the values of G_s/G_{max} obtained in the test series conducted at constant $\dot{\gamma}$ (ranging again between 0.0001 %/sec and 0.003 %/sec) consistently decrease with γ_c, just like for sands. The values of G_s/G_{max} obtained for clay in the test series conducted at constant frequencies of 3 and 0.3 Hz first increase with γ_c and then decrease. Such cyclic behavior occurs because if $f = \dot{\gamma}/(4\gamma_c)$ is constant, $\dot{\gamma}$ increases with γ_c, causing soil to respond as stiffer. These trends are also discussed in [8, 13, 9].

The effects of frequency, *f*, on λ were studied with the help of DSDSS device [14, 10]. The test results revealed that for many soils λ is in general the smallest at around $f \approx 0.1$ Hz. At larger *f*, λ is usually increasing with *f*, and below it usually decreases with *f*. Such a trend is consistent with some data presented earlier [15].

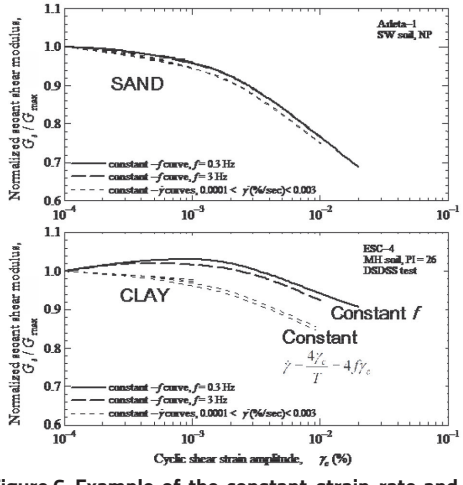

Figure 6. Example of the constant-strain-rate and constant-frequency normalized modulus reduction curves for sandy soil and clayey soil [10]

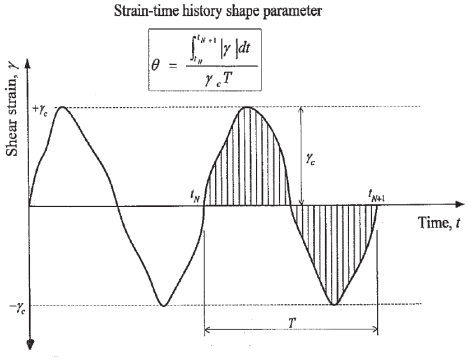

Figure 7. Definition of the strain-time history shape parameter, θ, measuring the effect of the shape of cyclic straining on the equivalent viscous damping ratio, λ [16]

The variation of the rate of straining in a single cycle affects damping λ and is associated with the fact that a longer application of larger strains in a single cycle allows for more relaxation and creep, which is generating larger area of the loop and thus larger damping λ. This means that for a given γ_c the area of the loop can be correlated to the

absolute area under the strain-time curve. On the basis of that, a parameter called the *strain-time history shape parameter*, θ, was defined [16], as shown in Figure . 7. For triangular cyclic straining θ =0.50, for sinusoidal θ =0.64, and for trapezoidal θ ≈ 0.75. The correlation between θ and λ for kaolinite clay tested at small λ_c is presented in Figure . 8. It is evident that changing the shape of cyclic straining can change λ dramatically.

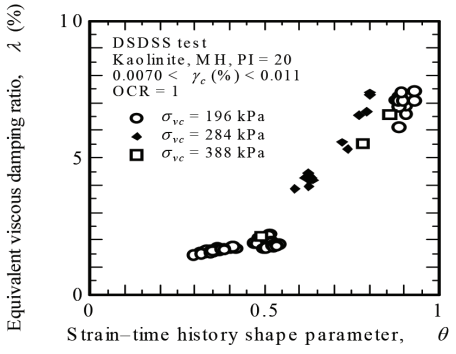

Figure 8. Trend of damping ratio, λ with the strain-time history shape parameter θ in the range of γ_c from 0.007 % to 0.011 % [10]

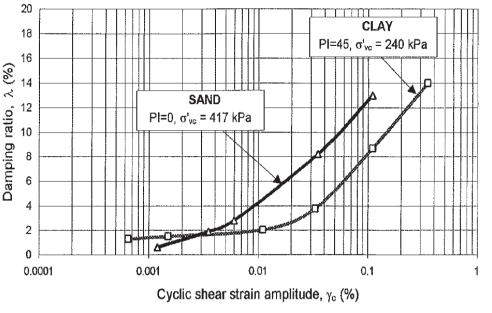

Figure 9. Damping curves λ-logγ_c for sand and clay obtained for sinusoidal cyclic straining crossing each other between γ_c =0.001 % and 0.01 % [14]

The above effects of the shape of cyclic straining are pronounced in soils that are more susceptible to creep and relaxation. They are small to negligible in clean sands and gravels and relatively large in clayey soils and generally increase with PI. This means further that the tips of the loops of clean sands are usually pointed, regardless of the shape of cyclic straining, while the tips of the loops of clay due to sinusoidal straining are rounded [17, 18, 19]. This has interesting consequences for the shape and relative position of the λ-logγ_c damping curves for clays with respect to those for sands [20]. Due to the roundness of the tips of the loops at small γ_c and difference in nonlinearity between sands and clays at large γ_c [21], the damping curves of sand and clay cross each other in the zone between γ_c≈0.001 % and 0.01 % [20], such as shown in Figure . 9. See also [22].

3 Threshold strains for cyclic degradation and pore water pressure in Clays

Threshold strains for cyclic degradation, γ_{td}, and cyclic pore water pressure, γ_{tp}, are fundamental cyclic soil properties [23]. If in clayey soil $\gamma_c<\gamma_{td}$ the soil does not degrade, δ_N= $G_{SN}/G_{S1}=\tau_{cN}/\tau_{c1}$ practically does not change. If $\gamma_c>\gamma_{td}$ index δ_N decreases with N such as shown in Figure 11 for the loops presented in Figure 10. Figure 12 shows thow the corresponding dergradation parameters, representng the slopes of the lines in Figure 11, t=logδ_N/logN, changes with γ_c. From this Figure γ_{td}=0.012 % can be derived.

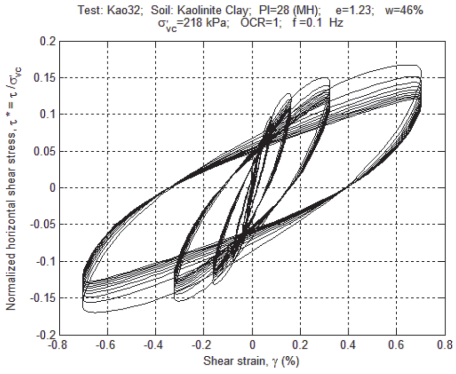

Figure 10. Stress-strain loops from cyclic strain-controlled simple shear tests on kaolinite clay [24, 25]

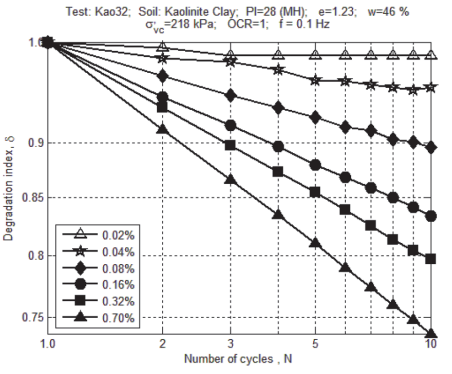

Figure 11. Cyclic degradation in the cyclic strain-controlled tests on kaolinite clay [24, 25]

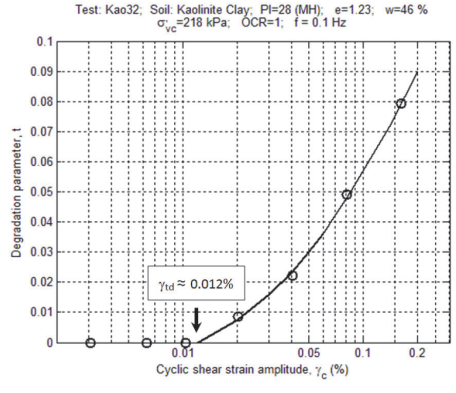

Figure 12. Variation of the degradation parameter, t, with the cyclic shear strain amplitude, γ_c [24, 25]

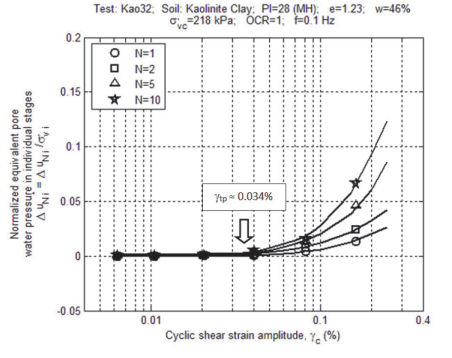

Figure 13. Change of the cyclic pore water pressure Δu_N^* with γ_c in the cyclic strain-controlled tests on normally consolidate kaolinite clay [24, 25]

Figure 13 shows the change of normalized cyclic pore water pressure $\Delta u_N^* = \Delta u_N / \sigma_{vc}'$ with γ_c for the tests results presented in Figure 10, where Δu_N is the pore water pressure at the end of cycle N. From this Figure γ_{tp}=0.034 %. Accordingly, from the same test results γ_{tp} is greater than γ_{td}. Such difference between γ_{td} and γ_{tp} obtained for many soils is displayed in Figure s 14 and 15.

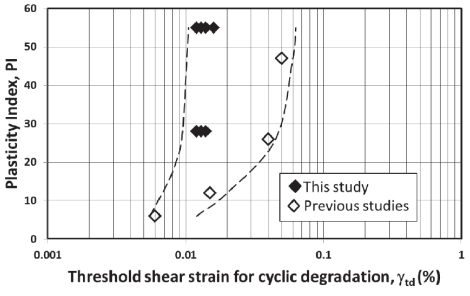

Figure 14. Relationship between the threshold shear strain for cyclic degradation, γ_{td}, and soil's plasticity index, PI [composed from 10, 24, 25, 26]

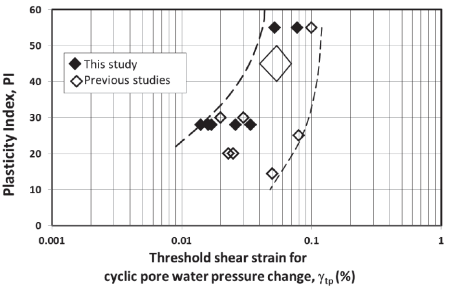

Figure 15. Relationship between the threshold shear strain for cyclic pore water pressure change, γ_{tp}, and soil's plasticity index, PI [24, 25]

4 Cyclic secant shear modulus and pore water pressure change in sands at small cyclic strains

Figure 16 shows the recent results of tests equivalent to those presented in Figure 10, but conducted on saturated sand instead of clay. They reveal that at the cyclic shear strain amplitudes, γ_c, between 0.01 % and 0.10 to 0.15 % the secant shear modulus at cycle N, G_{SN}, first increases with N, for up to 10 % of the initial G_{S1}, and then decreases, while the cyclic pore water pressure, Δu_N, monotonically increases, and that Δu_N can actually reach up to 40 % of the initial effective vertical stress before G_{SN} drops below G_{S1} and sands start to truly degrade [24, 27, 28, 29]. They also demonstrate that the effective stress principle, to the extent that it stipulates that if the pore water pressure increases during cyclic loading and the effective stress decreases, the sand stiffness and strength must decrease, is not universally valid. This should have significant impact on the analyses of the liquefaction seismic site response.

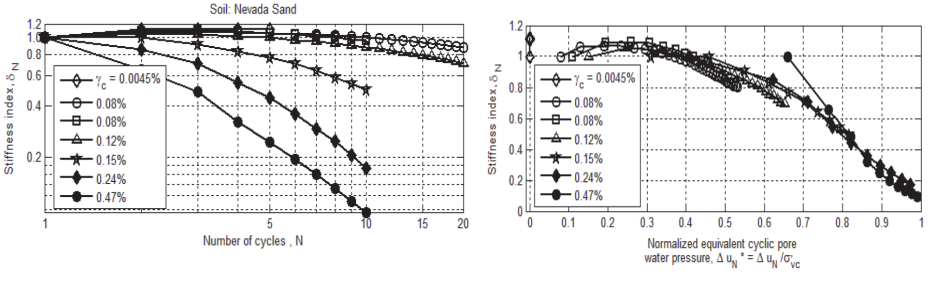

Figure 16. Variation of stiffness index, δ_N, with the number of cycles, N, and its relationship with cyclic pore water pressure, Δu_N^*, obtained in the simple shear cyclic strain-controlled tests on Nevada sand [24, 27]

5 Conclusions

The results presented in this paper and correspoding references obtained relatively recently, in particular the results in section 4 above, show that there are still fundamental aspects of the cyclic behavior of soils that need to be tested and clarified. They also ndicate that seismic site response models can be more accurate if recent discoveries are incorporated in their inputs. After decades of experimetal reserch, the high quality laboratory cyclic testing of soils, especially at small cyclic strains, is still a basic tool for the advancement of our understanding of the effects of earthquakes on civil engineering structures.

References

[1] Bjerrum, L., Landva, A. (1966): "Direct Simple-Shear Test on a Norwegian Quick Clay", Géotechnique, 16(1), 1-20. Cavallaro, A. (1997), "Influenza della velocità di deformazione sul modulo di taglio e sullo smorzamento delle argille". PhD Thesis. Università degli Studi di Catania, Italy.

[2] Doroudian, M., Vucetic, M. (1995): "A Direct Simple Shear Device for Measuring Small-Strain Behavior," ASTM Geotechnical Testing Journal, Vol. 18. No. 1, pp. 69-85.

[3] Doroudian, M., Vucetic, M. (1998): "Small-Strain Testing in an NGI-type Direct Simple Shear Device", Proceedings of the 11th Danube-European Conference on Soil Mechanics and Geotechnical Engineering, Porec, Croatia, Editors: Maric, B., Lisac, Z. and Szavits-Nossan, A., Publisher: A.A. Balkema, Rotterdam/Brookfield, pp. 687-693., May.

[4] Schnabel, P.B., Lysmer, J., Seed, H.B. (1972), "SHAKE: A Computer Program for Earthquake Response Analysis of Horizontally Layered Sites", Rept. EERC 72-12, Earthquake Engineering Research Center, University of California, Berkeley, CA.

[5] Lee, M.K.W., Finn, W.D.L. (1978): "DESRA-2 – Dynamic Effective Stress Response Analysis of Soil Deposits with Energy Transmitting Boundary including Assessment of Liquefaction Potential", Research Report, The University of British Columbia, Faculty of Applied Science.

[6] Vucetic, M., Dobry, R. (1986): "Pore Pressure Buildup and Liquefaction of Level Sandy Sites During Earthquakes," Report No. CE-86-03, Civil Engineering Department, Rensselaer Polytechnic Institute, Troy, New York, 660 p.

[7] Matasovic, N., Vucetic, M. (1993): "Seismic Response of Composite Horizontally-Layered Soil Deposits," UCLA Research Report No. ENG-93-182, Civil Engineering Department, University of California, Los Angeles, CA, March, 452 p.

[8] Isenhower, W.M., Stokoe, K.H. (1981): Strain-Rate Dependent Shear Modulus of San Francisco bay Mud", Proc. International Conference on Recent Advances in Geotechnical Earthquake Engineering and Soil Dynamics, University of Missouri - Rolla, 597-602.

[9] Matesic, L., Vucetic, M. (2003): "Strain-rate Effects on Soil Secant Shear Modulus at Small Cyclic Strains", ASCE Journal of Geotechnical and Geoenvironmental Engineering, Vol. 129, No. 6, pp. 536-549.

[10] Tabata, K., Vucetic, M. (2004): "The Effects of the Rate of Loading and Frequency on the Behavior of Soils at Small Monotonic and Cyclic Shear Strains", UCLA Research Report No. ENG-04-251, Civil and Environmental Engineering Department, University of California, Los Angeles, CA, November, 289 p.

[11] Vucetic, M., Tabata, K. (2003): "Influence of Soil Type on the Effect of Strain Rate on Small-strain Cyclic Shear Modulus", Soils and Foundation, Vol. 43, No. 5, pp. 161-173.

[12] Vucetic, M., Tabata, K., Matesic, L. (2003): "Effect of Average Straining Rate on Shear Modulus at Small Cyclic Strains" Proceedings, International Conference "Deformation Characteristics of Geomaterials", Lyon, France, Editors: Di Benedetto, H. et al., Publisher: A.A., Balkema, Lisse/ Abingdon/Exton/Tokyo, pp. 321-328.

[13] Santucci de Magistris (2002): "Effetto della velocita' di deformazione sul comportamento non lineare di una sabbia limosa", Incontro Annuale dei Ricerkatori di Geotecnica 2002 – IARG 2002, Napoli, Italy, 19-21 Giugno 2002.

[14] Lanzo, G., Vucetic, M. (1999): "Effect of Soil Plasticity on Damping Ratio at Small Cyclic Strains", Soils and Foundations, Vol 39, No. 4, pp. 131-141.

[15] d'Onofrio (1996): "Comportamento meccanico dell'argilla di Vallericca in condizioni lontane dalla rottura", PhD Thesis, Universita degli Studi di Catania.

[16] Vucetic, M., Lanzo, G., Doroudian, M. (1998b): "Effect of the Shape of Cyclic Loading on Damping Ratio at small Strains," Soils and Foundations, Vol. 38, No. 1, pp. 111-120.

[17] Vucetic, M. (1986): "The Stress-Strain Behavior of an Offshore Clay under Irregular Cyclic Simple Shear Loading," Report No. CE-86-02, Civil Engineering Department, Rensselaer Polytechnic Institute, Troy, New York, 81 p.

[18] Vucetic, M. (1990): "Normalized Behavior of Clay under Irregular Cyclic Loading," Canadian Geotechnical Journal, Vol. 27, No. 1, pp. 29-46.

[19] Dobry, R., Vucetic, M. (1987): "State-of-the-Art Report: Dynamic Properties and Response of Soft Clay Deposits," Proceedings of the International Symposium on Geotechnical Engineering of Soft Soils, Mexico City, Editors: Mendoza, M.J. and Montanez, L, Publisher: Sociedad Mexicana de Mecanica de Suelos, Mexico City, August, Vol. 2, pp. 51-87.

[20] Vucetic, M., Lanzo, G., Doroudian, M. (1998a): "Damping at Small Strains in Cyclic Simple Shear Test", ASCE Journal of Geotechnical and Geoenvironmental Engineering, Vol. 124, No.7, pp.585-594.

[21] Vucetic, M., Dobry, R. (1991): "Effect of Soil Plasticity on Cyclic Response," ASCE Journal of Geotechnical Engineering, Vol. 117, No. 1, pp. 89-107.

[22] Stokoe, K.H., Hwang, S.H., Lee, J.N.-K., Andrus, R.D. (1995): Effects of various parameters on the stiffness and damping of soils at small to medium strains, Proc. the First International Conference on Pre-failure Deformation Characteristics of Geomaterials, Sapporo, Japan, 1994: "Pre-failure Deformation of Geomaterials," A.A. Balkema, 785-816.

[23] Vucetic, M. (1994a): "Cyclic Threshold Shear Strains in Soils," ASCE Journal of Geotechnical Engineering, Vol. 120, No. 12, pp. 2208-2228.

[24] Mortezaie, A.R. (2012): "Cyclic threshold strains in clays versus sands and the change of secant shear modulus and pore water pressure at small cyclic strains", Ph.D. Thesis, Civil and Environmental Engineering Department, University of California, Los Angeles, May, 242 p.

[25] Mortezaie, A.R., Vucetic, M. (2016): "Threshold shear strains for cyclic degradation and cyclic pore water pressure generation in two clays", ASCE Journal of Geotechnical and Geoenvironmental Engineering, May 2016, 142 (5): 04016007, 14 p.

[26] Tabata, K., Vucetic, M. (2010): "Threshold Shear Strain for Cyclic Degradation of Three Clays", Proceedings of the Fifth International Conference on Recent Advances in Geotechnical Earthquake Engineering and Soil Dynamics, On CD-ROM, Session 1a, Paper No. 1.15a, San Diego, California, Publisher: Missouri University of Science and Technology, 12 pages.

[27] Vucetic, M., Mortezaie, A. (2015): "Cyclic Secant Shear Modulus versus Pore Water Pressure in Sands at Small Cyclic Strains", Soil Dynamics and Earthquake Engineering, Vol. 70, March 2015, pp. 60-72.

[28] Thangavel, H. (2019): "Relationship between the pore water pressure buildup and the change of stiffness in sands subjected to uniform and variable small to moderate cyclic shear strains", M.Sc. Thesis, Civil and Environmental Engineering Department, University of California, Los Angeles, 198 p.

[29] Vucetic, M., Thangavel, H., Mortezaie, A. (2021): "Cyclic Secant Shear Modulus and Pore Water Pressure Change in Sands at Small Cyclic Strains, ASCE Journal of Geotechnical and Geoenvironmental Engineering, DOI: 10.1061/(ASCE)GT.1943-5606.0002490

[30] Hashash, Y.M.A., Musgrove, M.I., Harmon, J.A., Groholski, D.R., Phillips, C.A., Park, D. (2016) "DEEPSOIL 6.1, User Manual". Urbana, IL, Board of Trustees of University of Illinois at Urbana-Champaign.